Performance Optimization and Instability Study in Ring Cavity Quantum Cascade Lasers

M. Moradinasab[1], M. Pourfath[2,1], O. Baumgartner[1], and H. Kosina[1]
[1]Institute for Microelectronics, TU Wien, Gußhausstraße 27–29/E360, 1040 Wien, Austria
[2]School of Electrical and Computer Engineering, University of Tehran, Tehran, Iran
Email: moradinasab@iue.tuwien.ac.at

***Abstract*—We present an optimization study of ring cavity quantum cascade lasers with regard to the instability condition. The effects of saturable absorber and pumping strength on the instability threshold are investigated using an analytical model. A numerical calculation based on the Maxwell-Bloch equations is performed to analyze the optimized structure.**

I. Introduction

Quantum cascade lasers (QCLs) are the most prominent and compact coherent light source in the wavelength range from 3.5 to 20 μm. The dynamics of QCLs is important for generating ultrashort pulses [1]–[3]. Unlike conventional semiconductor lasers, QCLs have a faster gain recovery (in the order of picoseconds) than the cavity round trip, owing to the ultrafast tunneling and intersubband electron-phonon scattering. Thus, in typical QCLs, self-mode-locking dominated by the saturable absorber (SA) effect is not possible, which spurs the mystery of the dynamic behaviors of QCLs [4]. It is demonstrated that the fast gain recovery of the QCLs exhibits two kinds of instabilities in the multimode regime: one is the Risken-Nummedal-Graham-Haken (RNGH)-like instability and the other is associated with spatial hole burning (SHB) [5]. Both RNGH and SHB instabilities are demonstrated in Ref. [6]. The SHB instability doesn't appear in ring cavity lasers where the standing wave, which is a requirement for this kind of instability, is absent.

In this work, we perform an optimization study of ring cavity QCLs with regard to the instability threshold. We employ the particle swarm optimization (PSO) method to maximize the gain and stable laser operation simultaneously by modifying the laser structure.

II. Model and Method

PSO is an evolutionary computation technique developed by Kenney and Eberhart [7]. It optimizes a problem by iteratively trying to improve a candidate solution with regard to a given measure of quality. This method is found to be robust in solving continuous nonlinear optimization problems [8]. Generally, the PSO method can be used to solve many problems of the same kind as genetic algorithm methods, and it can generate high-quality solutions with stable convergence characteristics, requiring only a concise program code [8]. Due to the large number of simulations needed for our study, we employ a computationally efficient semi-classical Monte-Carlo simulator based on the Pauli master equation [9].

The optimizer iteratively improves the reference structure by modifying the wells, the barriers widths, and applied electric field to achieve the maximum gain and laser operation below the instability threshold. The linear stability model introduced in Ref. [6] is employed to analyze the instability of the studied QCL. In this analytical formalism, the parametric gain $g(\Omega)$ as a function of the resonance frequency Ω provides the criterion for the characteristics of the RNGH instability.

$$g(\Omega) = -\frac{c}{2n}\mathrm{Re}\Bigg[l_0\frac{(\Omega T_1+i)\Omega T_2-2(p-1)}{(\Omega T_1+i)(\Omega T_2+i)-(p-1)}+ \frac{\gamma\hbar^2(p-1)}{\mu^2 T_1 T_2}\frac{(\Omega T_1+i)(3\Omega T_2+2i)-4(p-1)}{(\Omega T_1+i)(\Omega T_2+i)-(p-1)}\Bigg], \quad (1)$$

here p is the pumping factor, T_1 is the gain recovery time, T_2 is the dephasing time, l_0 is the linear cavity loss, μ is the matrix element of the lasing transition, and γ is the SA coefficient. For each mode identified by the resonance frequency Ω, the mode is stable for positive values of the parametric gain, and the mode is unstable for negative values. At each iteration, for a set of geometrical parameters and the applied electric field, a Monte-Carlo simulation is performed and the parameters $T_1,\ T_2,$ and μ are extracted. Based on these parameters, the parametric gain (Eq. 1) is evaluated. If the stability criterion is not satisfied, the optimizer selects a new set of parameters for the next iteration. Employing this approach, a modified stable structure with maximum laser gain is achieved.

III. Results and Discussion

The schematics of the conduction bands and wavefunctions of a reference design and optimized design are shown in Fig. 1. The layer sequence of the $\mathrm{In_{0.52}Al_{0.48}As/In_{0.53}Ga_{0.47}As}$ for the optimized structure, starting with the injection barrier is: **1.03**/3.34/**3.39**/3.64/**3.04**/<u>4.16/**2.39**/4.00/**4.50**</u>/2.98/**4.93**/3.56 /**3.7**/2.30/**1.71**/4.45 nm, where the barrier layers are in bold and the underlined layers are n-doped with Si at $2\times10^{17}\mathrm{cm}^{-3}$. The parameters used for instability analysis of the optimized structure are shown in Table I. Fig.2-a shows that the instability threshold increases uniformly with the SA coefficient. The parametric gain of the optimized structure at various pumping strengths is shown in Fig. 2-b. The results indicate that a larger

TABLE I. The parameters used for instability analysis of the optimized structure.

T_1	Gain recovery time	0.67 ps
T_2	Dephasing time	0.047 ps
μ	Matrix element of lasing transition	2.21×10^{-9} m
n	Refractive index	3.3
l_0	Linear cavity loss	500 m^{-1}
L	Cavity length	3×10^{-3} m
γ	Saturable absorber coefficient	10^{-11} $\mathrm{m/V^2}$

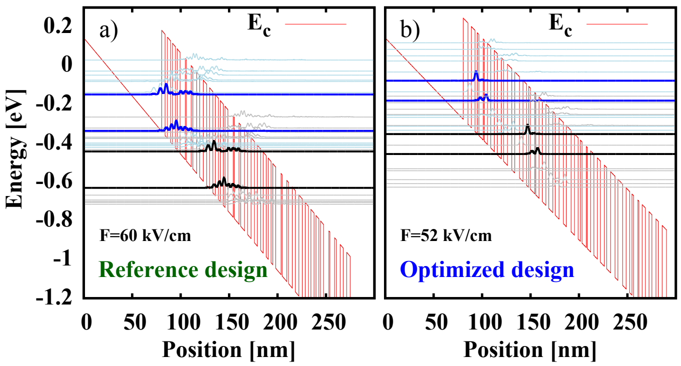

Fig. 1. The conduction band diagram and wavefunctions of (a) the reference design and (b) the optimized design. The lasing subbands are indicated with bold solid lines.

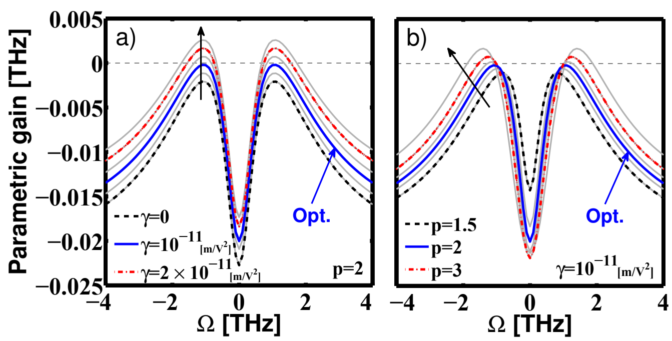

Fig. 2. The parametric gain $g(\Omega)$ as a function of the resonance frequency Ω at various (a) SA coefficients and (b) pumping strengths.

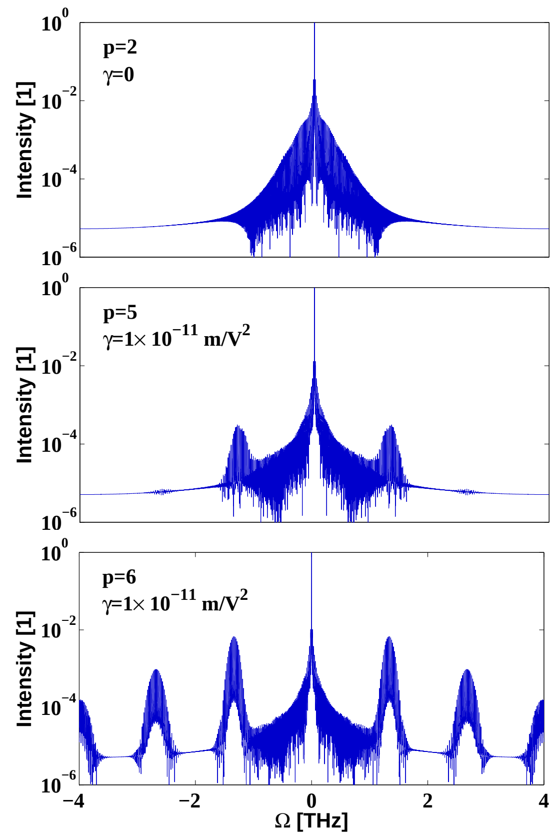

Fig. 3. The spectra of the optical intensity at various SA coefficients. The parameters of the simulated design are: $T_1 = 0.67$ ps, $T_2 = 0.37$ ps, $l_0 = 500$ m^{-1}, $\mu = 2.21 \times 10^{-9}$ m, $n = 3.3$, $L = 3 \times 10^{-3}$ m, $\gamma = 10^{-11}$ m/V^2.

pumping strength broadens the instability characteristics and decreases the instability threshold.

The linear stability analysis, however, predicts only the instability threshold and does not describe the dynamics of the laser. To investigate the dynamics of QCLs, we numerically solved the Maxwell-Bloch equations [6], employing the finite-difference discretization scheme in space and time domain. The effect of the SA is modeled as the intensity-modulated optical field amplitude.

For the parameters corresponding to the optimized QCL, including the SA, the lasing instability appears as the rise of the side modes with the increase of the SA coefficient. In lasers with slow gain recovery time, the transition in the Rabi sidebands is discontinuous [10], however, because of the fast gain recovery time in QCLs, Rabi sidebands continuously grow around the central cw mode, see Fig. 3.

Furthermore, more Rabi side modes appear with the increase of pumping strength.

IV. Conclusion

The performance optimization and instability in ring cavity QCLs are studied in this work. An optimization framework is developed to maximize the gain of the laser with regard to the instability threshold. The modification for a reference QCL sample with maximum performance and stable operation is achieved.

We investigated the SA and pumping strength effects on the instability threshold. The results indicate that the instability threshold increases uniformly with the SA coefficient. Moreover, the instability threshold in QCLs is lower than that of the RNGH instability in conventional lasers.

The numerical results based on the Maxwell-Bloch equations show that the lasing instability, exhibited as the side modes in the optical spectrum, appears either with the increase of the SA coefficient or higher pumping strength at the same SA coefficient.

Acknowledgment

This work has been partly supported by the Austrian Science Fund, special research programme F025 (IR-ON) and the European Seventh Framework Programme, contract 263306 (NanoHiTEC).

References

[1] J. M. Dudley *et al.*, Rev. Mod. Phys. **78**, 1135 (2006).
[2] R. Paiella *et al.*, Applied Physics Letters **77**, 169 (2000).
[3] R. Paiella *et al.*, Science **290**, 1739 (2000).
[4] J. Bai, Journal of Nanophotonics **4**, 043519 (2010).
[5] J. Bai, IEEE Trans. Nanotechnol. **11**, 292 (2012).
[6] A. Gordon *et al.*, Phys. Rev. A **77**, 053804 (2008).
[7] J. Kennedy *et al.*, in *Int. Conf. on Neural Networks* **4**, 1942 (1995).
[8] Z. L. Gaing, in *Power Eng. Soc. General Meeting, 2003, IEEE* **1**, (2003).
[9] O. Baumgartner *et al.*, in *Proc. SISPAD* 91 (2011).
[10] H. Haken *et al.*, Opt. Communications **26**, 117 (1978).